Structural Engineering and Mechanics, Vol. 31, No. 2 (2009) 211-223
DOI: http://dx.doi.org/10.12989/sem.2009.31.2.211

On the extended period of a frequency domain method to analyze transient responses

Kui Fu Chen†

College of Sciences, China Agricultural University, Beijing 100083, P.R. China

Qiang Zhang‡

Architecture Engineering School, Shanghai Normal University, Shanghai 201418, P.R. China

Sen Wen Zhang‡†

The Institute of Applied Mechanics, Jinan University, Guangzhou 510632, P.R. China

(Received October 25, 2006, Accepted December 17, 2008)

Abstract. Transient response analysis can be conducted either in the time domain, or via the frequency domain. Sometimes a frequency domain method (FDM) has advantages over a time domain method. A practical issue in the FDM is to find out an appropriate extended period, which may be affected by several factors, such as the excitation duration, the system damping, the artificial damping, the period of interest, etc. In this report, the extended period of the FDM based on the Duhamel's integral is investigated. This Duhamel's integral based FDM does not involve the unit impulse response function (UIRF) beyond the period of interest. Due to this fact, the ever-lasting UIRF can be simply set as zero beyond the period of interest to shorten the extended period. As a result, the preferred extended period is the summation of the period of interest and the excitation duration. This conclusion is validated by numerical examples. If the extended period is too short, then the front portion of the period of interest is more prone to errors than the rear portion, but the free vibration segment is free of the wraparound error.

Keywords: transient response; frequency domain method; fast fourier transform (FFT); laplace transform; Duhamel's integral; linear time invariant system.

1. Introduction

Dynamic analysis by computers, generally, can be achieved by discretizing governing equations, and then solving these discrete equations numerically. There exist several forms of describing a linear system, such as, the ordinary differential equations (ODE), multiplication in the frequency domain (FD), and convolution in the time domain (TD)—Duhamel's integral. Different forms of control equations lead to different algorithm families. Well-known algorithms of discretizing ODE

† Associate Professor, Corresponding author, E-mail: chenkuifu@gmail.com
‡ Associate Professor, E-mail: zhq@shnu.edu.cn
‡† Professor, E-mail: tzhsw@jnu.edu.cn

include the Runge-Kuta scheme, Wilson-theta scheme, Newmark-beta scheme, etc. Utilizing multiplication in the FD is based on the Fourier Transform (FT) or Laplace Transform theory, and practical computation makes use of the Fast Fourier Transform (FFT). This family is conventionally termed the frequency domain method (FDM) (Hall 1982, Chen and Zhang 1999, Moulinec and Suquet 2003, Kargarnovin and Younesian 2004, Polyzos *et al.* 2005).

FDMs possess inherent advantages in understanding the system behavior. First, the multiplication operation in the FD looks simpler than the ODE expression. This simple expression can facilitate both qualitative analysis and approximate computation. Second, concepts in the FD have a straightforward relationship with the FFT. Third, there are some systems containing infinite degrees of freedom. These systems pose difficulty, if not impossible, by solving ODE numerically, since we can not numerically solve equations with infinite orders. But, they may be comprehensive and solvable in the FD if the transfer function (or frequency response function) is known.

Usually, the FDM is derived from ODE expressions, which will be reviewed briefly in section 2. The essential concept is the extended period (Veletsos and Ventura 1984, 1985). The FDM can be built on the Duhamel's integral too, which is the topics of section 3. With this method, the ever-lasting unitary impulse response function (UIRF) can be truncated to shorten the extended period. Numerical examples will be examined in section 4.

2. FDM derived from ODE

2.1 Applying laplace transform to ODE

The governing equation of a linear vibration system with n degrees of freedom is

$$[M]\{\ddot{x}\}+[C]\{\dot{x}\}+[K]\{x\} = \{f(t)\} \tag{1}$$

Here $[M]$, $[C]$ and $[K]$ are $n \times n$ symmetrical matrices. They stand for the mass, damping and stiffness matrix, respectively. $\{f(t)\}$ and $\{x(t)\}$ are the $n \times 1$ excitation and response vectors, respectively. $[C]$ can be of either proportional damping or non- proportional damping, but must ensure that the system is stable. Transient analysis focuses on the short-lasting $\{f(t)\}$, such as an earthquake excitation. Denoting the duration of $\{f(t)\}$ as T_d.

Contribution of initial conditions is very important (Gupta *et al.* 1996, Siqueira Meirelles and Arruda 2005), but it is beyond the scope and aim of this report. For the sake of simplicity, zero initial conditions are assumed, that is, $\{x(0)\} = \{0\}$, $\{\dot{x}(0)\} = \{0\}$.

Applying the Laplace Transform to both sides of Eq. (1) and utilizing its differential properties lead to the following algebraic equation

$$s^2[M]\{X(s)\}+s[C]\{X(s)\}+[K]\{X(s)\} = \{F(s)\} \tag{2}$$

Here

$$\begin{cases} \{X(s)\} = \int_0^{\infty}\{x(t)\}e^{-st}dt \\ \{F(s)\} = \int_0^{\infty}\{f(t)\}e^{-st}dt = \int_0^{T_d}\{f(t)\}e^{-st}dt \end{cases} \tag{3}$$

are the Laplace Transforms of $\{x(t)\}, \{f(t)\}$, respectively. In light of Eq. (2), $\{X(s)\}$ can be read as

$$\{X(s)\} = [H(s)]\{F(s)\} \tag{4}$$

Here

$$[H(s)] = [s^2 M + sC + K]^{-1} \tag{5}$$

is the transfer function matrix. The interested $\{x(t)\}$ in the time domain can be retrieved out by the following inverse Laplace Transform

$$\{x(t)\} = \frac{1}{2\pi j}\int_{c-j\infty}^{c+j\infty} \{X(s)\} e^{st} ds \quad c \geq c_0 \tag{6}$$

Here real number c_0 is the convergence abscissa, that is, all the singular points locate on the left to Re(s) = c_0. Let us introduce the unitary impulse response function (UIRF) matrix [$h(t)$]-- the inverse Laplace Transform of [$H(s)$]

$$[h(t)] = \frac{1}{2\pi j}\int_{c-j\infty}^{c+j\infty} [H(s)] e^{st} ds = \frac{1}{2\pi j}\int_{c-j\infty}^{c+j\infty} [s^2 M + sC + K]^{-1} e^{st} ds$$

Combining Eq. (4) and Eq. (6) leads to

$$\{x(t)\} = \frac{1}{2\pi j}\int_{c-j\infty}^{c+j\infty} [H(s)]\{F(s)\} e^{st} ds \tag{7}$$

Eq. (6) only needs the data along the straight line Re(s) = c, thus only the integrand value along Re(s) = c is relevant, although s is defined over a two-dimension complex plane. If we choose $c = 0$, then all the Laplace Transform operations reduce to those of the FT, and Eq. (7) is as follows

$$\{x(t)\} = \frac{1}{2\pi}\int_{-\infty}^{\infty} [H(j\omega)]\{F(j\omega)\} e^{j\omega t} d\omega \tag{8}$$

Theoretically, analytically solving Eq. (7) or Eq. (8) renders a closed-form solution. But, computers favor numerical operations, especially when the FFT is employed to speed up Eq. (7) or Eq. (8). When continuous integrals are approximated by numerical versions, several practical considerations confront us, such as:

1) How does the integration scheme affect the accuracy?
2) How does the sampling point distribution along Re(s) = c affect the accuracy of numerical version of Eq. (8)?
3) How [$H(s)$] can be achieved efficiently? [$H(s)$] correlates with the system matrix by Eq. (5), but the matrix inverse for a great deal of s is much involved.

2.2 Extended period

Regarding the FT approach, a practical issue is specifying an appropriate extended period T_e. T_e is a finite time interval truncated by a FDM algorithm to compute the approximate Fourier transform.

In FFT, this extended period T_e has a relationship with the frequency interval $\Delta\omega$ as $\Delta\omega = 2/T_e$.

Veletsos (1984) had shown that the size of T_e is crucial, particularly for a lightly damped system. For example, for a single-degree-of-freedom (SDOF) system with a damping ratio $\zeta = 0.01$, T_e needs to be as 200 times as the natural period T_N to achieve four significant figures (digits) of peak displacements. The lighter of the damping, and the longer T_N, the larger T_e is needed, which entails a heavy computation burden. Moreover, even in theory, it can not work for the undamped case, since it necessitates an infinite T_e (Kausel and Roeosset 1992).

Empirical criteria to choose T_e for an SDOF system were suggested by several authors. The criteria proposed by Humar *et al.* (1993) is equivalent to

$$T_e = \beta \times 2\pi T_N / \zeta \times \ln 10 \tag{9}$$

where ζ is the damping ratio, T_N, the natural period, and $2 \le \beta \le 4$. Rule of thumb is that T_e has to be longer than the summation of two durations, the duration covering excitation, and the duration covering the significant non-zero part of a UIRF (2006), where the significant degree depends on the final accuracy and experience.

To reduce T_e, Veletsos *et al.* superimposed two correction functions onto the approximate results from Eq. (8). By this technique, T_e can be reduced dramatically. The closed-form correction functions for the SDOF case can be found in Veletsos and Ventura (1984). For the system with multiple degrees of freedom, these authors also provided numerical methods to construct correction functions.

2.2 Artificial damping and laplace transform

The critical issue of T_e is that UIRFs may be too long, which is also reflected by Eq. (9). Specifically, a light damping necessitates a long T_e. This inspires some authors to add an artificial damping to UIRF (Humar and Xia 1993, Hall and Beck 1993), which is also termed the exponential window method (Wang *et al.* 2001). This justifies the concept of the Laplace Transform. The Laplace Transform is a classical approach to analyze a transient response, especially in the case of seeking a closed-form solution.

The numerical Laplace Transform and its inversion are preferred by computers, since the closed-form solution is not feasible in a complex case. Several approximate approaches had already been proposed to implement the numerical Laplace Transform. Initially, the intimate relationship between the numerical FT and Laplace Transform was not much emphasized (Historically, Laplace Transform approaches to transient analysis numerically were developed independently of the FT approaches). This relationship was not recognized until the FFT was invented (Cooley and Tukey 1965) and applied to the numerical Laplace Transform (Durbin 1974, Yonemoto *et al.* 2003). Currently, the numerical Laplace Transform has found wide application in many engineering problems, e.g., crack and fracture analysis (Wang *et al.* 2001, Maeso *et al.* 2004), magneto (or electro)-thermoelasticity, material properties, transient analysis, heat transfer, thermal stress, chemical engineering and probability analysis, etc.

In the Laplace Transform expression Eq. (8), the role of the parameter c is the artificial damping. Empirical criteria to choose this parameter was suggested by Humar (1993) as $c = \ln 100/T_e \approx 4.61/T_e$, by Hall (1993) as $c = \ln 1000/T_e \approx 6.91/T_e$, and by Beskos (1983) as $c = 5/T_e \approx 10/T_e$.

3. FDM based on Duhamel's integral

3.1 Applying laplace transform to Duhamel's integral

Introducing a $2n \times 1$ vector $\{\phi\} = \begin{Bmatrix} \{\dot{x}\} \\ \{x\} \end{Bmatrix}$, then Eq. (1) can be read as

$$\{\dot{\phi}\} = [\Psi]\{\phi\} + \{r(t)\} \tag{10}$$

Here $[\Psi] = \begin{bmatrix} -M^{-1}C & -M^{-1}K \\ I & 0 \end{bmatrix}$, $\{r(t)\} = \begin{Bmatrix} [M]^{-1}\{f\} \\ 0 \end{Bmatrix}$. The mass, damping and stiffness matrices in Eq. (1) are assumed to be constant, therefore Eq. (10) is the mathematical representation, in the state form, of a linear time invariant (LTI) system. In light of the property of the LTI system, the solution of Eq. (10) under zero initial conditions is

$$\{\phi(t)\} = \int_0^t [\Xi(t-\tau)]\{r(\tau)\}d\tau \tag{11}$$

Here $[\Xi(t)]$ is the exponential matrix as follows

$$[\Xi(t)] = e^{[\Psi]t} = \exp\left(\begin{bmatrix} -M^{-1}C & -M^{-1}K \\ I & 0 \end{bmatrix} t\right) \tag{12}$$

It can be argued that integral bounds of Eq. (11) can be extended as follows (see appendix)

$$\{\phi(t)\} = \int_{-\infty}^{\infty} [\Xi(t-\tau)]\{r(\tau)\}d\tau \tag{13}$$

Applying the Laplace Transform to both sides of Eq. (13) leads to

$$\{\Phi(s)\} = (sI - [\Psi])^{-1} \begin{Bmatrix} [M]^{-1} \\ 0 \end{Bmatrix} \{F(s)\} \tag{14}$$

Here $\{\Phi(s)\}$ is the Laplace Transform of $\{\phi(t)\}$. It is easy to verify that

$$(sI - [\Psi]) \begin{bmatrix} s[H(s)][M] & -[H(s)][K] \\ [H(s)][M] & s[H(s)][M] + [H(s)][C] \end{bmatrix} = \begin{bmatrix} I & 0 \\ 0 & I \end{bmatrix} \tag{15}$$

Substituting Eq. (15) in Eq. (14), the lower half of $\{\Phi(s)\}$ is exactly the Eq. (4). This is taken for granted, since the Duhamel's integral Eq. (11) is simply another way to describe the identical system.

3.2 Differences between two methods

There are some differences about the premises and resulted computational procedures between algorithms based on the ODE and the Duhamel's Integral. The premises of Eq. (8) include all the nodes in the system, that is, all the system matrices $[M], [C], [K]$ must be provided, and the outputs cover the displacement trajectories at all nodes.

In the Duhamel's integral, $[\Xi(t-\tau)]$ can be any function, and can be of arbitrary dimensions, so

is Eq. (4). The purpose of correlating $[\Xi(t-\tau)]$ with $[M],[C],[K]$ via Eq. (12) is only for showing that two approaches of deriving the FDM are consistent. However, $[\Xi(t-\tau)]$ may not be of $2n \times 2n$ dimensions. In addition, it may have not explicit relationship with system parameters as Eq. (12). For example, the response can be computed from Eq. (12) or Eq. (4) without resorting to all the system parameters, if only the transfer function from the driving point to the interested node, along with the excitation, are provided. This is applicable to the single-input-single-output case of a system with multiple degrees of freedom, that is, a system is excited at only one point, and only the response on one point is interested.

There is no doubt, if the system parameters are provided, the transfer function is determined. However, the transfer function can be derived via other ways, such as, modal experiment analysis, or theoretical extension.

3.3 Achieving transfer function and UIRF

The modal experiment analysis is feasible if the original structures or laboratory models are available. Many approaches have already been developed to identify modal parameters. In the modal analysis community, much effort is cast on the parameter identification. Concerning the transient response from Eq. (12) or Eq. (4), a nonparametric UIRF or transfer function is sufficient.

The transfer function can also be derived from theoretical analysis, e.g., structures with unbounded media, including those that involve wave motion in reservoirs of large extent and unbounded solid media, and cracks development. For soil-structure interaction analysis, very often, soil is modeled as a homogeneous component with infinite boundary, or the spatial distribution of the material property is described by a simple expression with a few indexes. The interested structure above ground is discretized by a finite element method. The interaction between the infinite boundary component and interested structure can be described relatively easily by the transfer function in the frequency domain, because of the simple expression of the material property, and infinite boundary. This transfer function can be achieved by the boundary element method (olyzos *et al.* 2005, Liu and Huang 2003, Dumont and Oliveira 2001, Humar *et al.* 1998), or more specifically, scaled boundary finite-element method, or infinite element (Kim and Yun 2003, Song and Wolf 2000, Yan *et al*. 2004, Genes and Kocak 2005). Another highlighted approach to achieve the transfer function is the transfer matrix method, which is appropriate for structures containing repeated substructures (Xue 1997, Aleyaasin *et al*. 2001).

Theoretical extension of a transfer function usually involves the damping contribution. Very likely, this is due to the sophisticated damping mechanism. From the theory of classical mechanics, we know why the inertia and elastic forces are as they are, but the same is not exactly true for damping. Unlike the inertia and elastic forces, it is not much clear how the relevant state variables affect the damping forces (Adhikari 2002). A physically realizable system must be real and causal. The real requirement can be achieved by requiring that the extended frequency response function (the transfer function along the imaginary axis) must be conjugate symmetrical to the origin. However, the causal condition is not easily satisfied, such as the frequently cited hysteretic damping (Barkanov 1999, Inaudi and Kelly 1995, Makris and Zhang 2000, Tsai and Lee 2002, Chen and Zhang 2008). This argument is also applicable to models with frequency-dependent parameters, which frequently occur in soil-structure and fluid-structure interaction systems.

Obviously, the nonparametric transfer function derived from the experiment modal analysis necessitates a high order ODE to approximate it. Moreover, the transfer function derived from

theoretical analysis, or modification may have not a corresponding LTI system with a finite order (The modified transfer function may look simple, and have only tiny difference from the original ones, for example the hysteretic damping (Barkanov 1999, Inaudi and Kelly 1995, Makris and Zhang 2000, Tsai and Lee 2002, Chen and Zhang 2008)). Finite numerical operations are difficult, if not impossible, to solve an infinite order ODE.

However, the Duhamel's integral can circumvent these issues, because, firstly, just as aforementioned, the transfer functions may be concise. Secondly, from an engineering view, very often, the responses at some crucial points (not the entire system) are interested. For example, in the soil-structure interaction problem, the responses interested are the displacements and the stresses in the structure. The ODE approaches need all the system parameters, and yield the responses at all entire nodes in the system. In contrast, the Duhamel's integral is more specific, and only the transfer functions or the UIRFs between the excited points and interested points are necessary.

3.4 Truncating infiniteness

Examining Eq. (11), we can see that, for a specified t_0, $\{\phi(t_0)\}$ depends explicitly on $[\Xi(t)]$ on the period $[0, t_0]$, but not $(t_0, +\infty)$. In theory, for a linear structure, $[\Xi(t)]$ on $(t_0, +\infty)$ is determined by the value on $[0, t_0]$. But, from the view of computing $\{\phi(t_0)\}$ only, these two intervals can be manipulated independently. This is a very important property. Very often, from an engineering view, we are not so much interested in $\{\phi(t)\}$ on the whole time interval, for example, for the SDOF system, the maximum displacement occurs between the excitation beginning and one-half natural period T_N after the excitation stops, thus the interested interval is $(0, T_d + T_N/2)$ (Veletsos and Ventura 1984, 1985).

Assuming that $[0, T_I]$ is the period of interest, we can set $[\Xi(t)]$ arbitrarily in $(T_I, +\infty)$ without influencing the computational value $\{\phi(t)\}$ over $[0, T_I]$. A long T_e is due to the long-lasting UIRF. But, in light of the above property, we can set $[\Xi(t)]$ beyond $[0, T_I]$ as zero to reduce the T_e. This is just like the damping effect of the parameter c. Moreover, this perfect artificial damping just cuts down the UIRF piece over $[0, T_I]$ simply. In particular, this can be even applied to the extreme case, the undamped system.

The integral bounds of Eq. (8) are infinite, and must be truncated too. Assuming that both the excitation and UIRF are sampled uniformly with the sampling interval Δt. This discretization results in approximate versions to $\{F(j\omega)\}$ and $[H(j\omega)]$, which are periodic functions with a period $2\pi/\Delta t$. Obviously, Δt must be small enough, so that the fundamental period $(-\pi/\Delta t, \pi/\Delta t)$ can accommodate the principal spectrum parts, both for $\{f(t)\}$ and truncated UIRF $[h(t)]$. Under these assumptions, the infinite bounds of Eq. (8) are truncated to $(-\pi/\Delta t, \pi/\Delta t)$.

In brief, the equations involving in computation can be summarized as follows

$$\{F(j\omega)\} = \int_0^{T_d} \{f(t)\} \mathrm{e}^{-j\omega t} dt \tag{16}$$

$$[\hat{H}(j\omega)] = \int_0^{T_I} [h(t)] \mathrm{e}^{-j\omega t} dt \tag{17}$$

$$\{X(\omega)\} = [\hat{H}(j\omega)]\{F(\omega)\} \tag{18}$$

$$\{x(t)\} = \frac{1}{2\pi} \int_{-\pi/\Delta t}^{\pi/\Delta t} \{X(\omega)\} \mathrm{e}^{j\omega t} d\omega \tag{19}$$

where $[\hat{H}(j\omega)]$ is the FT of the truncated UIRF matrix $[h(t)]$. Eq. (16) and Eq. (17) are the forward transforms, and Eq. (19), the inverse transform, and all their numerical version can be speeded up by the FFT (Cooley and Tukey 1965). If the $[h(t)]$ is not provided, it must be retrieved from $[H(j\omega)]$ through the inverse Laplace Transform.

Such kind of truncating the UIRF is equivalent to substituting the system with an artificial system. This artificial system has the UIRF with a finite duration T_I. Thus, under an excitation with a duration T_d, the response duration of this artificial system is at most $T_d + T_I$. The essence of the discretization in the FD is periodically extending in the time domain, which correlates to the Fourier series analysis. To obtain the response accurately, the fundamental frequency, that is, the lowest frequency to mimic the response, must be not greater than $2\pi/(T_d + T_I)$. Otherwise, the responses can not be constructed accurately from its harmonics. This requires that $\Delta\omega \le 2\pi/(T_d + T_I)$, that is, $T_e \ge T_d + T_I$ should be satisfied, though we are only interested in the response on [0, T_I]. If either the truncated URIF, or the excitation, or both, approaches zero at their ends, then the time-limited artificial response at ends of the extended period is close to zero, which makes the artificial computational response shorter. As a consequence, T_e can be shorter than $T_d + T_I$.

4. Numerical examples

4.1 Model and computational parameters

The following SDOF system has been discussed extensively in literature

$$m\ddot{x} + c\dot{x} + kx = f(t)$$

or equivalently $\ddot{x} + 2\zeta\omega_n\dot{x} + \omega_n^2 x = f(t)/m$.

Here, m = 1 kg, $\omega_n = 2\pi$rad/s, (T_N = 1s) are used. The excitation $f(t)$ is as follows (T_d = 1.25s).

$$f(t) = \begin{cases} P\sin(\alpha \times 2\pi t) & 0 < t \le T_d \\ 0 & t > T_d \end{cases}$$

Here, α controls the excitation wave number. Three cases of α as α = 0.2, 0.8, 1.4, and two cases of the damping ratio ζ = 0.01, and ζ = 0.05 are considered.

The number of the force sampling points is selected as N_d = 64, as a result, $\Delta t = T_d/N_d$ = 1.25/64 s. Because the maximum displacement can occur only before $T_d + T_N$ /2 for an SDOF system, N_I=90 is selected. This number just ensures that the period of interest is $T_I = N_I\ \Delta t$ = 1.773 > $T_d + T_N$/ 2 = 1.75 s. We introduce the symbol $\delta N = N_I + N_d + 1 - N_e$, which is the paramount index to indicate wraparound interference (Chen and Zhang 2006). Eight cases of $\delta N = 8k$, k = 0~7 were examined. All the three integrals (Eq. (16), Eq. (17) and Eq. (19)) are solved using the composite rectangle rule, and speeded up by the FFT (Cooley and Tukey 1965). The closed-form UIRF is used. The exact transient response is

$$x(t) = Be^{-\zeta\omega_n t}\left(\sin\varphi\cos\sqrt{1-\zeta^2}\,\omega_n t + \frac{\zeta\omega_n\sin\varphi - 2\alpha\pi\cos\varphi}{\sqrt{1-\zeta^2}\,\omega_n}\sin\sqrt{1-\zeta^2}\,\omega_n t\right) + B\sin(2\alpha\pi t - \varphi) \quad (20)$$

The free response after T_d is

$$x(t) = e^{-\zeta\omega_n(t-T_d)} \times \left[x(T_d^-)\cos\sqrt{1-\zeta^2}\,\omega_n(t-T_d) + \frac{\dot{x}(T_d^-)+\zeta\omega_n x(T_d^-)}{\sqrt{1-\zeta^2}\,\omega_n}\sin\sqrt{1-\zeta^2}\,\omega_n(t-T_d) \right] \quad (21)$$

B and φ in Eqs. (20) and (21) are

$$B = \frac{\omega_n^2\delta_{\mathrm{st}}}{\sqrt{(4\pi^2\alpha^2-\omega_n^2)^2+(4\pi\zeta\alpha\omega_n)^2}}, \quad \varphi = \arctan\frac{4\pi\zeta\alpha\omega_n}{4\pi^2\alpha^2-\omega_n^2} \quad (22)$$

4.2 Results and discussion

Fig. 1 shows the computational results of the case: α = 0.2 and ζ = 0.01. Fig. 1(a) outlines the excitation, which is a quarter of a sine wave. The eight cases of δNs are presented in Fig. 1(b)~ Fig. 1(i) sequentially, where the dot and thin continuous line stand for the exact solution and computational results, respectively. The responses shown in (b)~(i) are normalized by a factor $x_{st} = P/k$, where x_{st} stands for the static displacement occurring when the constant force P, the peak force of the sinusoidal excitation, acts on the system.

The whole period of interest covers the expiation duration 0~T_d. and free response segment T_d.~

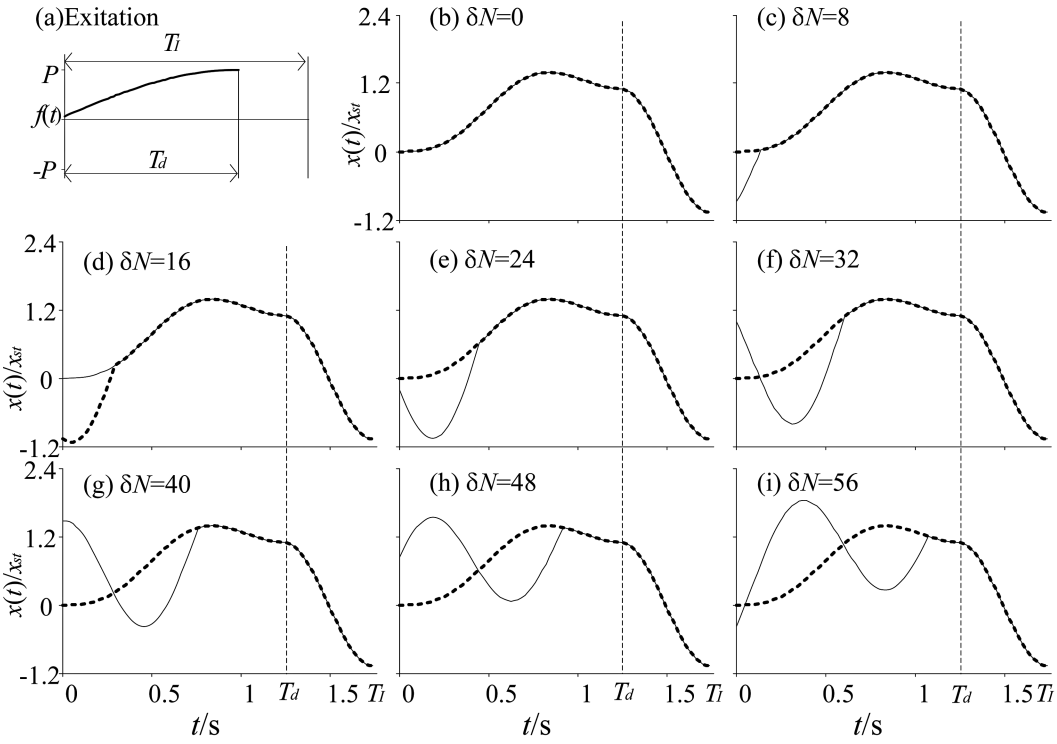

Fig. 1 The Influence of δN (α = 0.2 and ζ = 0.01). (a) outlines the excitation. (b)~(i) correspond to the 8 cases of δNs, where the dot and thin continuous lines stand for the exact solutions and computational results, respectively. Computational parameter δN influences computational responses dramatically.

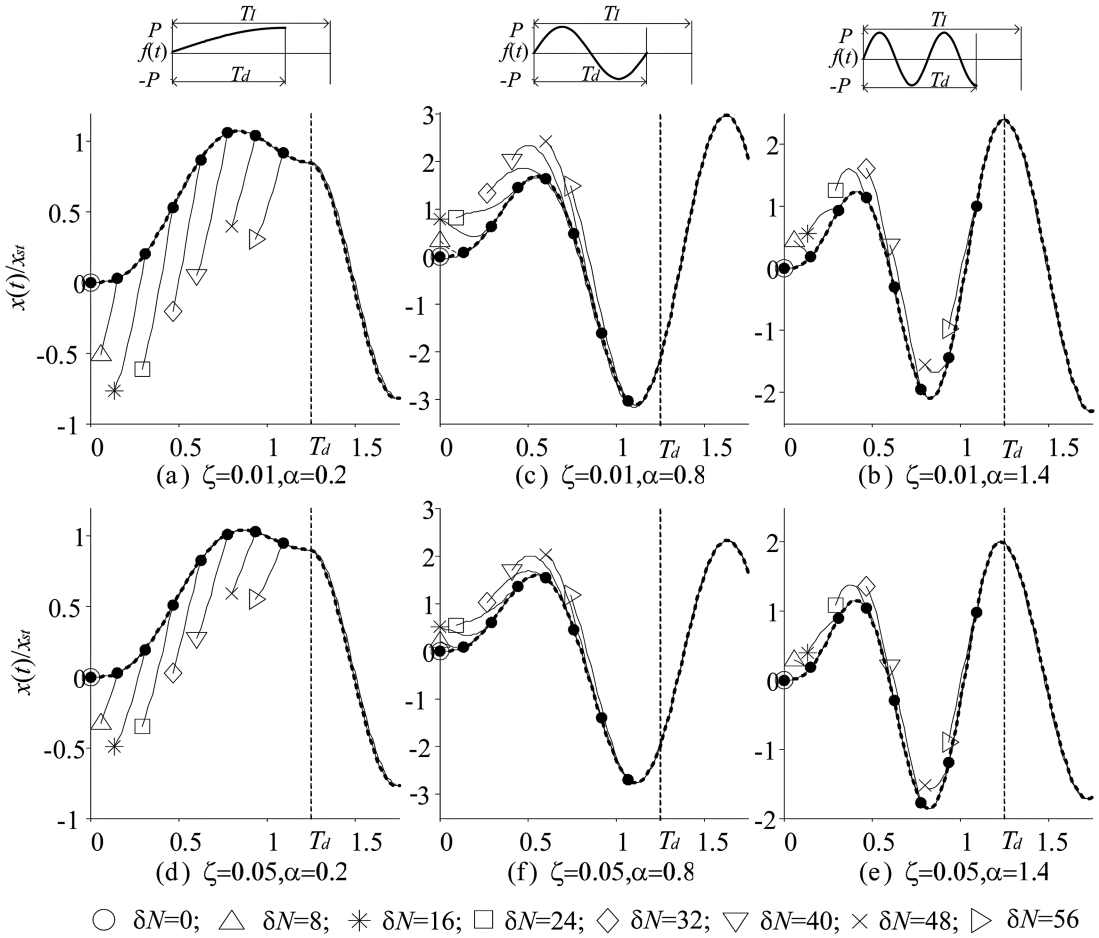

Fig. 2 Comparison between exact and computational displacements. For nonnegative δNs, the deviating positions of computational responses from the exact are depicted by dots along exact trajectory. For the sake of clarity, front parts of some computational responses are trimmed off.

T_I. The left sides to the vertical dash line are the forced responses, and the right sides, the free responses. We can see the computational responses of eight graphs match the exact solution over the free response segment. However, the forced responses are not always consistent. For $\delta N = 0$ of the graph (b), the computational result overlap with the exact response over all the period of interest. As δN increases, the former deviates from the latter at some point.

To argue more generally, the eight cases of computational responses of Figs. 1(b)~(i) are stacked in Fig. 2(a). Here markers at the left ends of the stubbed computational responses depict different cases of δN. Similarly, the results of other computational conditions are organized into Figs. 2(b)~(f). The figurine at the top of each column in Fig. 2 stands for the excitation waveform. All these graphs show that free vibration responses are consistent among all the simulated δN cases, overlap with the exact solution. The largest δN is $N_d + 1$, which occurs when N_I equals to N_e. That is, the extended period is equal to the period of interest. Even for this extreme case, simulation shows that the free response is still coincident with the exact version.

In contrast, the computational forced responses depend on the paramount index δN. The dots along the exact trajectories depict the distinct deviation instant of computational results from the corresponding exact responses. These deviating instants depend exclusively on δN. As δN decreases, the deviation positions move leftward, till $\delta N = 0$. When δN is zero, computational results on the whole period of interest overlap with the exact responses. If N_e is increased further, resulting in a negative δN, the computational results do not vary any longer on the period of interest.

Thus, $\delta N = 0$, that is, $N_e = N_I + N_d + 1$ is a reasonable solution to the extended period. It must be pointed out that N_I and N_d are the sampling interval numbers on the period of interest, and excitation periods, respectively. Their lengths are $N_I + 1$ and $N_d + 1$, respectively. In other word, $\delta N = 0$ requires that the extended interval number N_e equal to one less than the length summation of the excitation series and the truncated UIRF series. This agrees with qualitative analysis in Chen and Zhang 2006).

In the left column graphs, the abscissas of deviation points can be quantitatively expressed as $(N_I + N_d + 1 - N_e)\delta t = \delta N \Delta t$. The computational responses lying right to this position match with the exact ones, but not to the left. That is to say, computational results on the right side is reliable, and on the left, unreliable. The most significant contribution to the computational error of the left side is due to the wraparound inference (Chen and Zhang 2006). If we do not concern about the wraparound error occurring at the initial portion of $(0, T_I)$, N_e can be less than $N_I + N_d + 1$. For example, in an SDOF system with zero initial conditions, the maximum displacement can not appear at the very beginning, thus we can ignore the initial portion without causing eminent errors on the maximum displacement. Nonetheless, the duration of this initial portion need be selected judiciously.

In the central and right column graphs, we can see that computational responses deviate from the exact ones tangentially, which is contrast to the intercept-like way in the first and second columns. Tangential-like way renders the deviation positions ambiguously, particularly at the rear segment of the period of interest.

5. Conclusions

Frequency domain methods can be built on either the ordinary differential equation (ODE), or the Duhamel's integral. Two methods are equivalent, provided that all the system parameters are known, and the responses at entire nodes in the studying system are required. But there are several factors which make the Duhamel's integral method advantageous over the ODE method.

With the Duhamel's integral method, to shorten the extended period, the ever-lasting UIRF can be substituted by a truncated version, which is identical to the original version on the period of interest, and is zero beyond the period of interest. This approach, in theory, reduces the critical extended period to the summation of the period of interest and the excitation duration.

This criterion was confirmed by numerical examples. If the critical extended period is not long enough, then the front portion of the period of interest is more sensitive to the wraparound error than the rear portion, and the free vibration segment is free of wraparound error.

References

Adhikari, S. (2002), "Dynamics of nonviscously damped linear systems", *J. Eng. Mech.*, **128**(3), 328-339.

Aleyaasin, M., Ebrahimi, M. and Whalley, R. (2001), "Flexural vibration of rotating shafts by frequency domain hybrid modelling", *Comput. Struct.*, **79**(3), 319-331.
Barkanov, E. (1999), "Transient response analysis of structures made from viscoelastic materials", *Int. J. Numer. Meth. Eng.*, **44**(3), 393-403.
Beskos, D.E. and Narayann, G.V. (1983), "Dynamic response of frameworks by numerical laplace transform", *Comput. Method. Appl. M.*, **37**, 289-307.
Chen, K.F. and Zhang, S.W. (1999), "DFT acceleration and its application in non-stationary random vibration calculation", *Chinese J.Vib. Eng.*, **12**(1), 91-96.
Chen, K.F. and Zhang, S.W. (2006), "On the convergence and causality of a frequency domain method for dynamic structural analysis", *Acta Mech. Sinica*, **22**(2), 162-169.
Chen, K.F. and Zhang, S.W. (2008), "On the Impulse response precursor of an SDOF ideal linear hysteretic damper", *J. Sound Vib.*, **312**(4-5), 576-583.
Cooley, J.W. and Tukey, J.W. (1965), "An algorithm for the machine calculation of complex fourier series", *Math. Comput.*, **19**(90), 297-305.
Dumont, N.A. and Oliveira, R.D. (2001), "From frequency-dependent mass and stiffness matrices to the dynamic response of elastic systems", *Int. J. Solids Struct.*, **38**(10-13), 1813-1830.
Durbin, F. (1974), "Numerical inversion of Laplace transforms: an efficient improvement to Duber and Abate's method", *Comput. J.*, **17**(4), 371-376.
Genes, M.C. and Kocak, S. (2005), "Dynamic soil-structure interaction analysis of layered unbounded media via a coupled finite element/boundary element/scaled boundary finite element model", *Int. J. Numer. Meth. Eng.*, **62**(6), 798-823.
Gupta, A.K., Hassan, T. and Gupta, A. (1996), Time and frequency domain analyses of single-degree-of-freedom systems", *Nuclear Eng. Des.*, **167**(1), 1-5.
Hall, J.F. (1982), "FFT algorithm for structural dynamics", *Earthq. Eng. Struct. Dyn.*, **10**(6), 797-811.
Hall, J.F. and Beck, J.L. (1993), "Linear System Response by DFT: Analysis of a recent modified method", *Earthq. Eng. Struct. Dyn.*, **22**(7), 599-615.
Humar, J.L. and Xia, H. (1993), "Dynamic response analysis in the frequency domain", *Earthq. Eng. Struct. Dyn.*, **22**(1), 1-12.
Humar, J.L., Bagchit, A. and Xia, H. (1998), "Frequency domain analysis of soil-structure interaction", *Comput. Struct.*, **66**(2-3), 337-351.
Inaudi, J.A. and Kelly, J.M. (1995), "Linear hysteretic damping and the Hilbert transform", *J. Eng. Mech.*, ASCE, **121**(5), 626-632.
Kargarnovin, M. and Younesian, D. (2004), "Dynamics of Timoshenko beams on Pasternak foundation under moving load", *Mech. Res. Commun.*, **31**(6), 713-723.
Kausel, E. and Roeosset, J.M. (1992), "Frequency domain analysis of undamped systems", *J. Eng. Mech.*, ASCE, **118**(4), 721-734.
Kim, D.K. and Yun, C.B. (2003), "Earthquake response analysis in the time domain for 2D soil-structure systems using analytical frequency-dependent infinite elements", *Int. J. Numer. Meth. Eng.*, **58**(12), 1837-1855.
Liu, S.W. and Huang, J.H. (2003), "Transient dynamic responses of a cracked solid subjected to in-plane loadings", *Int. J. Solids Struct.*, **40**(18), 4925-4940.
Maeso, O., Aznarez, J.J. and Dominguez, J. (2004), "Three-dimensional models of reservoir sediment and effects on the seismic response of arch dams", *Earthq. Eng. Struct. Dyn.*, **33**(10), 1103-1123.
Makris, N. and Zhang, J. (2000), "Time-domain viscoelastic analysis of earth structures", *Earthq. Eng. Struct. Dyn.*, **29**(6), 745-768.
Moulinec, H. and Suquet, P. (2003), "Comparison of FFT-based methods for computing the response of composites with highly contrasted mechanical properties", *Physica B*, **338**(1-4), 58-60.
Polyzos, D., Tsepoura, K.G. and Beskos, D.E. (2005), "Transient dynamic analysis of 3-D gradient elastic solids by BEM", *Comput. Struct.*, **83**(10-11), 783-792.
Siqueira Meirelles, P. and Arruda, J.R.F. (2005), "Transient response with arbitrary initial conditions using the DFT", *J. Sound Vib.*, **287**(3), 525-543.
Song, C.M. and Wolf, J.P. (2000), "The scaled boundary finite-element method - a primer: Solution procedures", *Comput. Struct.*, **78**(1-3), 211-225.

Tsai, H.C. and Lee, T.C. (2002), "Dynamic analysis of linear and bilinear oscillators with rate-independent damping", *Comput. Struct.*, **80**(2), 155-164.
Veletsos, A.S. and Ventura, C.E. (1984), "Efficient analysis of dynamic response of linear-systems", *Earthq. Eng. Struct. Dyn.*, **12**(4), 521-536.
Veletsos, A.S. and Ventura, C.E. (1985), "Dynamic analysis of structures by the DFT", *J. Eng. Mech.*, ASCE, **111**(12), 2625-2642.
Wang, Y.Y., Lam, Y.K. and Liu, G.R. (2001), "A strip element method for the transient analysis of symmetric laminated plates", *Int. J. Solids Struct.*, **38**(2), 241-259.
Xue, H.Y. (1997), "A combined finite element-Riccati transfer matrix method in frequency domain for transient structural response", *Comput. Struct.*, **62**(2), 215-220.
Yan, J.Y., Zhang, C.H. and Jin, F. (2004), "A coupling procedure of FE and SBFE for soil-structure interaction in the time domain", *Int. J. Numer. Meth. Eng.*, **59**(11), 1453-1471.
Yonemoto, A., Hisakado, T. and Okumura, K. (2003), "Accuracy improvement of the FFT-based numerical inversion of Laplace Transforms", *IEE Proceedings-Circuits Devices and Systems*, **150**(5), 399-404.

Appendix: Proof of Eq. (13)

1) If $t \geq T_d$, then derivation from Eq. (11) to Eq. (13) is obvious, for $\{r(\tau)\}$ is nonzero only on $[0, T_d]$. Thus, expanding the integral bound does not change $\{\phi(t)\}$, that is

$$\{\phi(t)\} = \int_0^{T_d} [\Xi(t-\tau)]\{r(\tau)\}d\tau = \int_{-\infty}^{\infty} [\Xi(t-\tau)]\{r(\tau)\}d\tau \tag{A1}$$

2) If $t < T_d$ then Eq. (11) can be rewritten as

$$\{\phi(t)\} = \int_0^{T_d} [\Xi(t-\tau)]\{r(\tau)\}d\tau - \int_t^{T_d} [\Xi(t-\tau)]\{r(\tau)\}d\tau$$

For a causal system, due to $t < \tau$, the second term $[\Xi(t-\tau)]$ at the right is zero. Therefore, the above equation is exactly Eq. (A1).